

**MODELING AEOLIAN EROSION POTENTIAL ON MARS WITH THE MRAMS LES.** Michaels<sup>1</sup>, T. I. and Fenton<sup>1</sup>, L. K. and Michaels<sup>2</sup>, T. I. <sup>1</sup>Carl Sagan Center, SETI Institute; NASA Ames Research Center, lfenton@carlsagancenter.org, <sup>2</sup>Department of Space Studies, Southwest Research Institute, 1050 Walnut St., Suite 400, Boulder, CO 80302, tmichael@boulder.swri.edu.

**Introduction:** A significant goal of Mars science is to understand the present-day interaction between the atmospheric environment and the planet's surface that ultimately results in climatically- and geologically-important aeolian phenomena (*e.g.*, dust storms, dust devils, albedo changes, dune migration, and surface erosion). Although the potential impact of larger atmospheric flows on surface-atmosphere interactions has been studied at length with regional and global climate models (GCMs) [*e.g.*, 1-3], studies of simulations resolving the complex, highly three-dimensional dry convective circulations that produce dust-lifting events are still uncommon [*e.g.*, 4,5].

We present preliminary results of large eddy simulations (LES) on Mars. In order to produce results that are directly comparable from one region or season of Mars to another, we have used idealized wind profiles as initial conditions to the simulations, rather than those derived from a coarser (but perhaps more locally realistic) regional climate model domain. We demonstrate that wind "gustiness" (*i.e.*, the stronger intermittent winds produced by daytime convective turbulence) is dependent on both the time variation of insolation and the initial wind profile.

**MRAMS Large Eddy Simulations (LES):** The Mars Regional Atmospheric Modeling System (MRAMS) is a non-hydrostatic, finite-difference, limited domain mesoscale model [6,7]. It can perform LES when the subgrid scale turbulence is modified to explicitly model eddies down to the domain resolution, based on the method of [8]. The simulations were run under idealized conditions, such that the LES setup did not include topography and the domain had periodic boundary conditions to effectively simulate the atmosphere over a vast plain.

We have run several large eddy simulations at two locations on Mars: the approximate Viking Lander 1 (VL1) site (22.28° N, 312.05° E, elevation ≈ -3640 m) and Phoenix Lander site (68.21° N, 234.26° E, elevation ≈ -4130 m). Other than location and initial conditions inherited from mesoscale simulations, each LES was run with the same characteristics. The horizontal domain grid spacing was 100 m, spanning 24 km in each direction (240 x 240 grid points). The 99 vertical layers in the domain stretched in thickness from 4 m at the surface to 150 m near the top (at ~12 km). The dynamical time step was 1 s. Each simulation was run at  $L_s = 120^\circ$  (northern hemisphere summer), with a dura-

tion from approximately sunrise to sunset of a single day. In order to isolate the effects on the boundary layer convection due to differing wind profiles, we used three idealized wind profiles chosen for their relative simplicity. The three initial wind profiles were defined as follows:

*Case 1:* No initial wind,  $u(z,t=0) = 0$ ,  $v(z,t=0) = 0$

*Case 2:* Uniform wind,  $u(z,t=0) = 5$  m/s,  $v(z,t=0) = 0$

*Case 3:* Wind speed shear,  $u(z,t=0) \approx 1.46z+2$ ,  $v(z,t=0) = 0$ , (such that  $u(z=0) \approx 2$  m/s and  $u(z=12 \text{ km}) \approx 20$  m/s).

**Results:** In the Case 1, there is no mean wind, so that all wind gusts (measured here at the surface as high values of friction velocity) are produced solely by the development of buoyantly-induced turbulence within the convective boundary layer. One measure of insolation-driven buoyancy is the vertical potential temperature gradient at the surface ( $d\theta/dz$ , the surface static (in)stability): values less than zero indicate static instability, where the solar forcing has heated the surface more than the near-surface atmosphere, triggering dry convective turbulence that tries to equalize the energetic disparity between the two.

Figure 1 shows the distribution of surface static instability and friction velocity at ten local times across the VL1 domain. The surface air is statically unstable by midmorning, reaches a maximum level of static instability around local noon, and gradually grows less statically unstable as the afternoon progresses. By late afternoon (17.63h LMST), the sun is low in the sky and can no longer heat the surface enough to produce a negative vertical potential temperature gradient; at this point the convective boundary layer begins to collapse. Friction velocity distributions broaden throughout the morning and early afternoon, reflecting increased gustiness produced by buoyantly-driven turbulence within the boundary layer. The peak gustiness occurs in the early afternoon (12.63h – 14.63h LMST), shortly after the surface static instability has reached a maximum and the boundary layer has had time to react to this strong gradient with vigorous circulations. According to Mars lander observations, dust devil activity peaks in the early afternoon, consistent with our LES results [*e.g.*, 9,10].

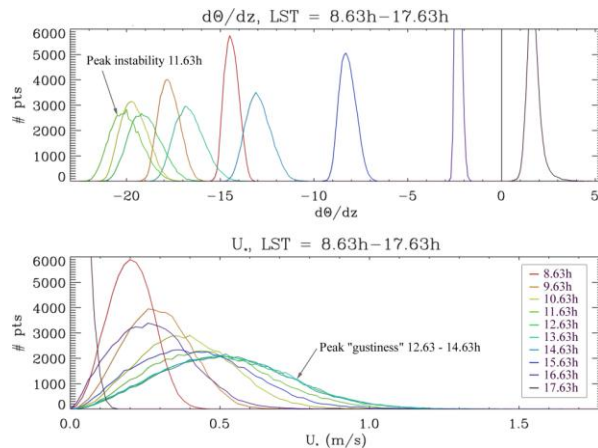


**Figure 1.** VL1 site, Case 1 domain distributions of surface instability and friction velocity in the morning and afternoon.

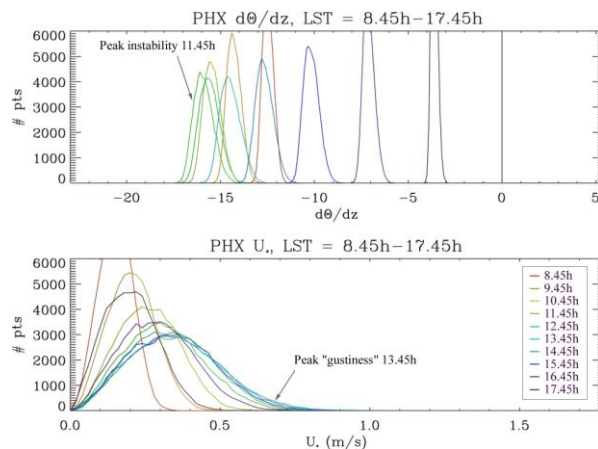


**Figure 2.** Phoenix site, Case 1 domain distributions of surface instability and friction velocity in the morning and afternoon.

Figure 2 shows similar plots of surface static stability and friction velocity at the Phoenix site. As at the VL1 site, instability at the Phoenix site reaches a maximum around local noon, although at such northern latitudes insolation is not direct enough to produce as strong a vertical potential temperature gradient. As the insolation decreases during the afternoon, the static instability decreases but much more slowly than at the VL1 site, since during the arctic summer the sun is above the horizon at all times. Thus the convective boundary layer at the Phoenix site may not produce such vigorous turbulence as that at the VL1 site, but buoyantly-driven turbulence takes longer to subside in the evening. This result is reflected in the distribution of friction velocities in Fig. 2, which never reach the same maxima as those at the VL1 site, but which take longer to weaken in the afternoon.

Results from Cases 2 and 3 indicate that the initial wind profile has a profound effect on wind distributions several hours later in the day. At both the VL1

and Phoenix sites, higher velocity initial winds lead to stronger peak winds relative to Case 1. At the VL1 site, buoyantly-driven turbulence dominates over wind-shear-driven turbulence from the initial wind structure during the hours of peak insolation. However, at the Phoenix site, convective activity is weaker, allowing the initial wind structure at the Phoenix site to more prominently influence the turbulence.

**Conclusions:** Large eddy simulations, using idealized initial wind profiles at two lander locations, have demonstrated that daytime convective turbulence can significantly increase the likelihood of particle entrainment on Mars, and that the degree of this enhancement is dependent on several factors. Wind gustiness generally increases with insolation, such that the strongest winds produced by convective turbulence would occur when the sun is highest in the sky, as dictated by local time and latitude.

The distribution of friction velocities is also dependent on the initial wind profile, which influences wind gustiness throughout the day and varies in impact with insolation and local time. Such imposed “mean wind” structures generally elevate peak friction velocities, increasing the likelihood that particle entrainment will occur. When the sun is high in the sky, convective activity reaches its peak and, if vigorous enough, can nearly override the initial wind structure.

The general nature of these relationships is not surprising, since conceptually, the nature of turbulence is determined by the relative strengths of two competing production terms: buoyant processes (tied to surface insolation) and mechanical processes (tied to wind shear). We intend to continue our study of simulated wind distributions and their effect on particle entrainment. Large eddy simulations at other locations (with varying elevation, albedo, and thermal inertia) and seasons will help to establish how these factors influence wind gustiness. Ultimately our goal is to develop a parameterization of the high tail of friction velocities for researchers to use as “perturbation” winds that can be superimposed on “mean” winds from mesoscale models, leading to estimates of particle entrainment on Mars that are more realistic.

**References:** [1] Toigo A.D. et al. (2002) *JGR*, 107(E7), doi:10.1029/2001JE001592. [2] Haberle R.M. et al. (2003) *IC*, 161, 66-89. [3] Armstrong J.C. and Leovy C.B. (2005) *IC*, 176(1), 57-74. [4] Toigo A.D. et al. (2003) *JGR*, 108(E6), doi:10.1029/2002JE002002. [5] Michaels T.I. (2006) *GRL*, 33, doi:10.1029/2006GL026268. [6] Rafkin S.C.R. et al. (2001) *IC*, 151, 228-256. [7] Michaels T.I. (2002) MSc thesis, San Jose St. Univ. [8] Deardorff J.W. (1980) *Bound.-Layer Meteorol.*, 18, 495-527. [9] Ellehøj et al. (2009) *LPS XL*, Abstract #1558. [10] Greeley, R. et al. (2006) *JGR*, 111, E12S09, doi:10.1029/2006JE002743.